Refractory Corrosion in Industrial Waste Incineration Processes

The aim of this work was the evaluation of corrosion mechanisms of different refractories in operation of waste incineration plants. A testing method in steam atmosphere according ASTM was used to determine the oxidation resistance. Different silicon carbide materials with amounts of Si_3N_4 and Si_2N_2O within their bonding phase composition were exposed to a constant steam flux at 900 °C with different time coordinates between 25 and 500 h. Since the same materials have been applied to industrial waste incineration plants an evaluation of the laboratory methods and the corrosion behaviour could be worked out and compared to the industrial performance of the bricks. Different established bonding phases have a strong influence on the oxidation behaviour resulting in micro- and macro-crack formation after application to corrosive steam environment. Different time dependant material behaviour for the volume change of the bricks was observed respectively.

Dr.-Ing. Thorsten Tonnesen
Prof. Dr. Rainer Telle
RWTH Aachen University, Institute of Mineral Engineering, Aachen, Germany
Corresponding author:
tonnesen@ghi.rwth-aachen.de

Introduction

In waste incineration plants refractories suffer different corrosion environments due to their specific application. Corrosion attack differs for the areas of air cooling, water cooling or insulating refractory lining. The design of the cooling for the lining has a direct influence on the choice of materials. Limitation parameters for the corrosion of the refractories are surface and vessel temperatures, dust in the hot gases as well as slag formation of molten ashes. The selective design of the vessel is mainly influenced by hot gas corrosion, oxidation and melt corrosion. Different refractory SiC materials are used for water cooling lining areas of side walls or pipe walls. SiC containing masses are chosen for filling gaps between brick lining and pipes. A particular choice of oxide and non-oxide materials is given for non cooling high temperature areas of a vessel.
Oxidation behaviour of refractory SiC was already examined in different studies [1, 2, 3]. A particular research was mainly done for the bonding phase. Commonly used nitride bonding phases with different amounts of α-Si_3N_4, β-Si_3N_4, Si_2N_2O und SiAlON have been tested according to their oxidation resistance in steam atmospheres [4, 5]. Degradation of the microstructure due to phase formation, crack formation or volume increases has a direct influence on thermo-physical properties resulting in a change of performance of an incineration plant lining (Figs. 1 and 2). Thermal expansion behaviour is one example. In this study different lining areas and different refractory corrosion mechanism are described and discussed.
The following materials and their range of application in waste incineration plants have to be distinguished:

- Nitride bonded refractory SiC, brick shapes for pipe walls and straights, lining areas with active cooling
- SiC refractory mortars and masses, lining areas with active cooling
- Shaped high alumina bricks with mullite bonding, non-cooling areas of the entrance area of a waste incineration vessel.

The following wear mechanisms are described more in detail:

- Oxidation mechanism of nitride bonding phase
- Microstructural changes of the refractory and following influences for the furnace operation conditions
- Influence of condensed species and corrosion of the microstructure within the porous mortar composition
- Phase formation and microstructural changes due to slag corrosion and changing of material properties such as thermal expansion

On one hand results originating from laboratory experiments are described as well as

Fig. 1 Nitride bonded SiC after operation in an industrial waste incineration plant: Slag formation at the hot face, oxidation and crack formation

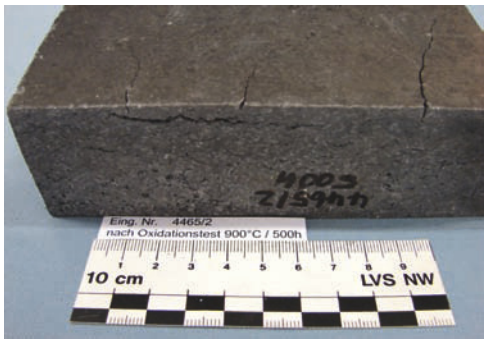

Fig. 2 Nitride bonded SiC after laboratory oxidation resistance test at 900 °C / 500 h: Crack formation and increase of volume

Table 1 Material properties of nitride bonded SiC specimens

SiC bricks			
Chemical composition / mass-%			
SiC		80,0 – 85,0	
Si_3N_4 + Si_2ON_2		17,0 – 23,5	
SiO_2		2,0	
Fe_2O_3		0,2 – 0,5	
Material	SiC A		SiC B
Bulk density / g/cm³	2,68		2,69
Open poriosty / %	13,42		15,45

Table 2 Material properties of SiC mortar after firing at 1000 °C

Type	Bulk density	Porosity	Phases	
	kg/m³	%	Major phase	Minor phase
SiC mortar	2,16	25,8	α-SiC	β-SiC
				Al hydrogen phosphate
				quartz (traces)
				kaolinite (traces)

Table 3 Chemical composition of high alumina refractory bricks as received

Type	High alumina refractory
Oxide	[mass %]
Al_2O_3	85,22
SiO_2	11,64
Fe_2O_3	0,24
TiO_2	0,21
CaO	0,01
MgO	0,11
K_2O	0,15
Na_2O	0,14
Cr_2O_3	0,01
P_2O_5	1,28
ZrO_2	1,00

post-mortem analyses of samples after operation under industrial conditions.

Experimental

Determination of the Bonding Type on the Oxidation Resistance of Nitride Bonded SiC

The examined materials are industrial products and are commonly used in waste incineration plants. To describe the influence of the bonding type on the oxidation resistance the SiC materials were tested according to ASTM C 863-83 (reapproved 1988) [6]. In particular nitride bonded silicon carbide materials were tested at 900 °C for maximum 500 h. For a better evaluation of the reaction mechanism the time coordinates were also kept variable so that the property changes were determined after different periods.

The as received properties of the used materials are given in Table 1. The SiC materials A and B have been produced at different times between 1991 and 2003 and have been applied in the same industrial waste incineration plant in Germany. New materials from these production periods have been used for these laboratory studies to evaluate the very different performance of the materials of one type but different performances in the same plant. Material A showed a very good performance with more than 56 000 h of operation. After this period no crack formation or other damages could be observed during inspection. Material B revealed a much shorter lifetime with less than 20 000 h of operation. Also spalling and crack formation after industrial operation had to be recognized. The use of new material for the laboratory studies knowing the lifetime in the plant should underline the feasibility of testing methods to work out the different resistance to such corrosive environments.

To characterize the oxidation resistance steam atmosphere with a constant rate of 32 kg/h per 1 m³ furnace size is used to accelerate the testing. Oxidation resistance is defined as the ability of silicon carbide materials to resist the formation of silica followed by crystal growth. Temperature dependant oxidation products are amorphous SiO_2 and cristobalite. The oxidation process is accompanied with a permanent expansion and a dramatic drop of the mechanical properties of the refractory material. The rate is mainly influenced by the amount of steam.

A special setting of the silicon carbide samples in the reaction chamber enables that nearly the whole surfaces of the samples are in contact to the steam. Following testing conditions were established:

- Heating of the furnace <2 K/min up to 900 °C
- Inflation of the steam atmosphere into the reaction chamber
- Testing times: 25, 50, 100, 150, 200, 250, 300, 350, 400 and 500 h
- Cooling of the furnace < 2 K/min

Before and after the testing following properties were determined to describe the oxidation resistance:

- Bulk density, determination of the sample volume
- Porosity and pore size distribution by mercury porosimetry
- Changes of weight and volume.

In particular the materials A and B were examined by SEM in as-received state and after 500 h exposure at the described conditions. The different oxidation behaviour is worked out.

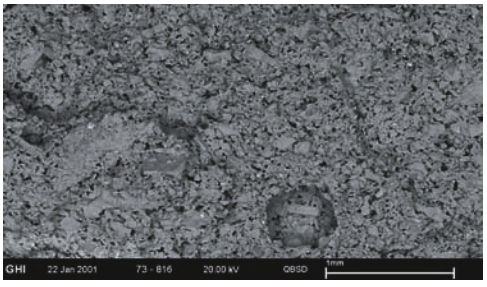

Fig. 3 SEM micrograph of SiC mortar as received

Corrosion Experiments of SiC Mortars

For the vapour phase corrosion experiments with evaporated salt mixtures conventional SiC containing mortars have been applied. Tab. 2 summarizes some technical and structural properties of the mortar. Fig. 3 gives an example of a typical mortar as received. Grog SiC grains as well as the homogeneous porosity can be examined very well. For the gas corrosion tests solid mixtures from KCl and $ZnCl_2$ with a ratio of 1:1 have been used. They were placed on prisms of the SiC mortar of the dimension 250 x 50 x 50 mm³. The corrosion temperature was 350 °C, annealing time was 350 h. A constant evaporation rate was achieved by changing the solid salt bodies after a certain time. The results of the microstructural changes due to the salt corrosion were examined by means of SEM.

Corrosion Experiments of Refractories in Direct Slag Contact

The refractory material applied in a non-cooling area of the entrance area of an industrial waste incineration furnace was a

high alumina refractory with ZrO_2 addition and a mullite bonding phase. The mineral composition was corundum (Al_2O_3) and mullite ($3\ Al_2O_3 \cdot 2\ SiO_2$) as a major phase and zircon ($ZrSiO_4$) in traces. As received a bulk density of 3.0 g/cm³ and an apparent porosity of 13 % have been analysed. The chemical composition of the bricks is given in Table 3. After slag corrosion phase and structural changes were observed by XRD. The changed microstructure was examined by SEM.

Results

Oxidation Resistance Behaviour

For an increase of the corrosive conditions and for an evaluation of the microstructural influence oxidation resistance tests have been performed on nitride bonded silicon carbide bricks at 900 °C. Steam rate was kept constant, the time coordinates were in a range between 25 and 500 h. Fig. 4 shows the achieved results for SiC material A and B at 900 °C for the different time coordinates. The different increase of the specimen volume of the nitride bonded materials A and B becomes obvious. The maximum values of the volume increase scatter between 2,04 % and 6,30 % after 500 h. The measurements at different time coordinates show a dramatic different slope of increase between the two materials. Between 150 and 200 h of testing the curves show different increases. SiC material A has just a moderate increase for the time between 200 and 500 h. For SiC material B the step increase is remarkable. After 200 h testing time the increase is constant and results in a maximum value of 6,30 % after 500 h. Macroscopic examinations after 250 h and 500 h oxidation test confirm the measured results of the increasing weight and volume of the samples A and B. Crack formation or shape deformation cannot be regarded for the samples with the lowest volume increase of 2,04 %. The silicon carbide samples with a higher gain in weight and volume show crack formations after 250 h at the edges. Crack opening stretch takes place and after 500 h crack formation along the width of the silicon carbide specimen has occurred. The testing time dependant crack branching within the microstructure becomes obvious in increasing absolute values for open porosity before and after testing as well as the pore size distribution shows remarkable differences. The porosity experiments show a decrease in porosity which already underlines differences of the oxidation behaviour. For SiC material A the value for porosity drops from 15,0 % to 13,8 % representing a small decrease after oxidation. For SiC material B a drop for porosity from 15,0 % to 10,9 % was achieved. Regarding the dia-

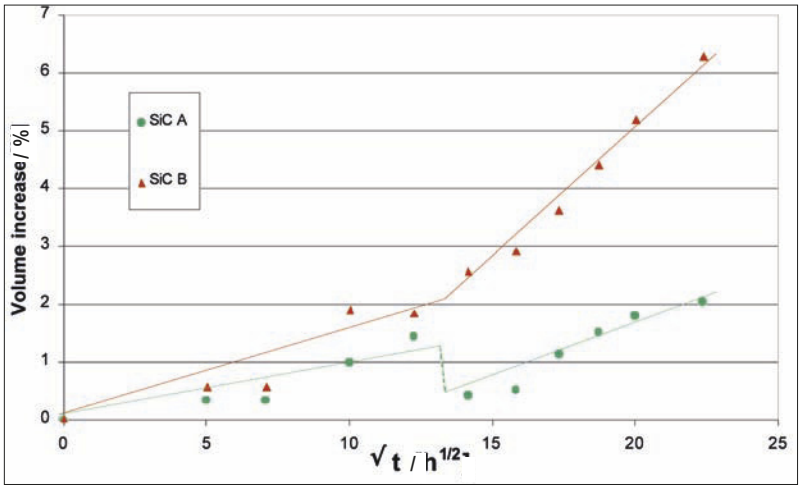

Fig. 4 Volume increase of nitride bonded SiC after oxidation resistance test at 900 °C

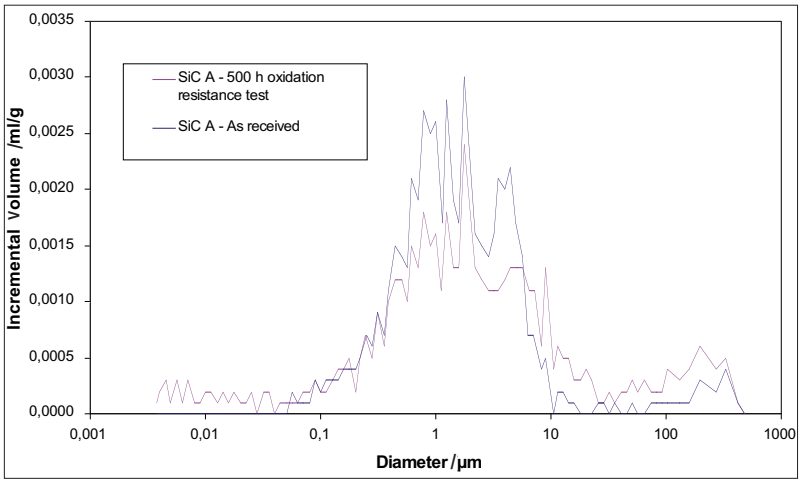

Fig. 5 Pore size distribution of SiC A before and after oxidation resistance test at 900 °C / 500 h

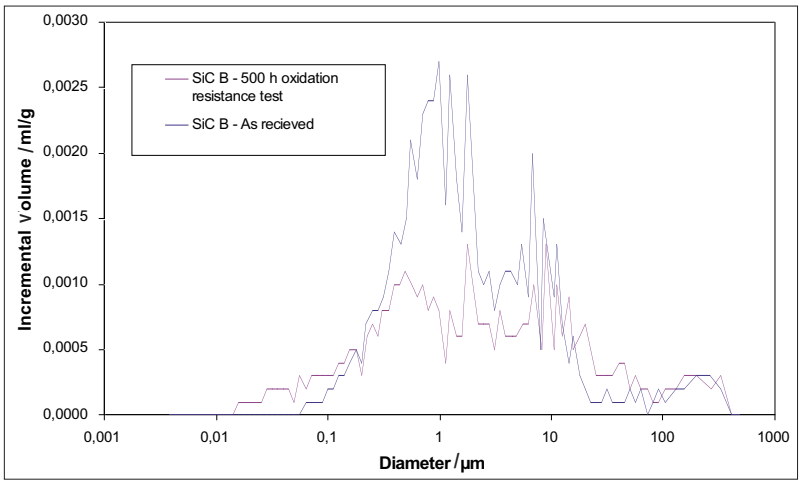

Fig. 6 Pore size distribution of SiC B before and after oxidation resistance test at 900 °C / 500 h

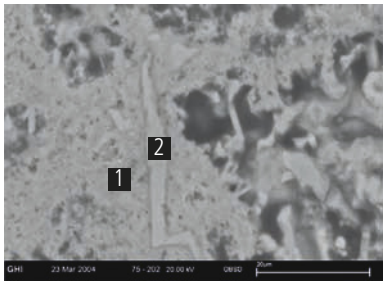

Fig. 7 SiC Material A, detail of the bonding phase of nitride bonded silicon carbide refractory after 500 h oxidation resistance tests at 900 °C (1 – Si-O-N phase (29 % N, 38 % Si), 2 - SiC)

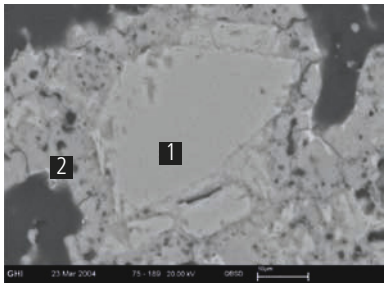

Fig. 8 SEM micrograph of the bonding phase of nitride bonded SiC type B after 500 h oxidation resistance test at 900 °C (1 - SiC; 2 - SiO_2)

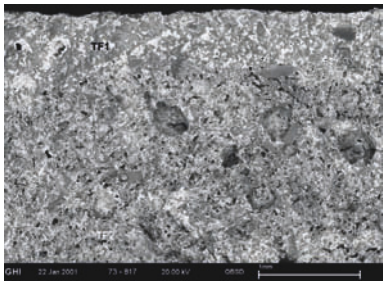

Fig. 9 Refractory SiC mortar after salt corrosion tests at 350 °C / 500 h, overview of different zones at the hot face

grams of the pore size distribution no change could be observed for material A (Fig. 5). On the other hand the amount of pores in the main range of 0,8 µm to 3 µm show a big deviation before and after the oxidation resistance test at 900 °C (Fig. 6). Crystallization of silica phase such as cristobalite has taken place consuming main volume of the open porous areas of this size. The change in the pore size distribution curve is obvious.

The results of the SEM analyses of the bonding phases of material A and B are given in Figs. 7 and 8. The homogenous distribution of the nitride phase of material A is obvious. The porosity is also distributed homogenous and an averaged pore diameter of 5 µm can be recognized. The grog silicon carbide grains are embedded and show small rims at the edges. Thus a passivating oxidation of the silicon carbide grains has occurred within the production process of the refractory. The microstructure of the material after 500 h oxidation test is partial determined by larger pores although the complete porosity does not differ a lot. The components of the binding phase suffer oxidation mechanisms in a different way. The formation of oxynitrides improves the oxidation resistance enormously. A complete oxidation accompanied by a massive SiO_2 formation does not occur in these microstructural parts of the silicon carbide material A. In regard of its oxidation resistance these microstructural areas are of great importance. A continuous Si-O-N-matrix has been formed. Crystallization and mainly oxide phase formations which may lead to severe volume expansion cannot be examined.

As received the microstructure of material B reveals a higher amount of larger pores. Porous rims are around the grog silicon carbide grains leading to a comparatively inhomogenous embedding of the grog grains into the matrix. Between open porous pipes of 20 µm diameter small bridges of silicon carbide bonding phase have been formed. It is remarkable that mainly carbides form the bonding phase within the microstructure. The SEM analysis of the bonding phase after the oxidation resistance test shows silicon carbide grains surrounded by a bonding phase consisting of SiO_2 (Fig. 8 [2]). A total transformation of the bonding phase into silica has taken place. Within this oxide phase single left silicon carbide grains with a size of 5 µm become obvious. Fine silicon carbide matrix is oxidised followed by the precipitation of silica-rich glassy phase. Crystallization of this glassy phase leads to micro crack formation. Due to crystal SiO_2 formation stresses within the microstructure have to be decomposed. This leads to an expansion of the microstructure and crack formation. Due to the lack of nitride compounds within the bonding phase mainly oxide phase is formed. In this case oxidation resistance is much lowered and the crack formation leads to decreasing physical properties respectively. Passivating influence of the SiO_2 formation is not achieved. Further an enlargement of the pores can be recognized.

The main factors for a different performance of these materials are given by the bonding phase within the matrix. Crystallization of silica phases such as cristobalite takes place within the porosity, leading to a lower porosity value and a differed pore size distribution. The silica rich phase within the bonding phase leads to microcrack formation. After the long term experiments the cracks grow, volume increase and macroscopic visible cracks are the consequence.

Corrosion by Salts

The effect of the corrosion experiments with KCl-$ZnCl_2$ salt mixtures on the refractory microstructure are given in Figs. 9 and 10. The open porous microstructure is totally penetrated by diffused and condensated species. At the boundary to the solid salt a densified zone of 600 µm can be recognized. The open pores are filled with salt species in total forming a dense layer. The related microstructure behind this zone shows also mechanisms of vapour phase corrosion but a residual porosity is still obvious (Fig. 9). The marked areas in the SEM micrograph reveal the same chemical composition. EDS analysis gives reaction product with 17,5 % Si, 15 % Cl, 6,5 % K, 6,6 % Zn, 4 % Al, 4 % P and 0,3 % V. Further it becomes obvious that open porous areas around grog SiC grains are totally filled with salt species forming a densified rim around the aggregates. At the cold face of the SiC mortar samples salt compounds could also be identified with lower intensity (Fig. 10). Nevertheless the diffusion paths along the pores are visible. Condensation of salt species and resulting crack formation in the matrix are also remarkable (Fig. 10). The added salt mixture of KCl and $ZnCl_2$ and its stoichiometry can be identified within macro pores.

Corrosion Behaviour after Slag Contact

Figs. 11 and 12 show SEM overview micrographs of polished high alumina refractory samples after operation in a non cooling area of the entrance area of an industrial waste incineration furnace. Sampling has

been performed at the hot face of the refractory. The microstructure was analysed starting at the hot face and continuing the analysis to the cold face of the polished section. The micrographs show sections of the refractory material in direct contact to the slag. The microstructure is densified and EDS analyses reveal the infiltration of the whole microstructure by slag. Fig. 7 identifies that the initial refractory composition has changed to a calcium alumosilicate. Precipitation of needle like anorthithe ($CaO \cdot Al_2O_3 \cdot 2\ SiO_2$) or anorthite facettes become obvious in Fig. 11 [2]. At the boundary the composition of the precipitated calcium alumosilicate is enriched with alkalis (Fig. 11 [1]). The sum of the Na_2O and K_2O is 6,6 %. Phases of the bonding are fused alumina needles, hercynite ($FeO \cdot Al_2O_3$) as well as small ZrO_2 crystals within porous areas between grog grains. The main composition of the bonding phase is a calcium alumosilicate with an anorthite like composition. The densification of the microstructure becomes obvious in the detailed SEM micrographs. The penetration of the microstructure is also remarkable observing the related microstructure of areas with lower temperatures (Fig. 12). The phases are more alumina rich revealing less CaO respectively. Fig. 12 also makes clear that related microstructure is more porous (Fig. 12 [TF2]). Penetration of the lime-rich slag leads to a complete infiltration and precipitation of calcium alumosilicates with an anorthite-like composition. With higher depth of the brick, lower temperatures and higher slag viscosity the chemical composition changes also resulting in a higher porosity. Further ZrO_2 compounds are still homogeneous distributed in these porous areas. Microstructure related to the hot face shows dissolution of the ZrO_2 compounds. Fig. 12 reveals also that the used zircon ($ZrSiO_4$) is still consistent. In hot face related microstructure decomposition according to the reaction $ZrSiO_4 \leftrightarrow ZrO_2 + SiO_2$ takes place. Single ZrO_2 grains can be identified in these areas. Alkalis from the slag have a favourable influence on this decomposition reaction. Examinations of the cold face underline that the samples have been totally penetrated by the slag since amounts of CaO are analysed. Furthermore the porosity is more similar to an original microstructure although the rims of the grog alumina grains already show some reaction zones.

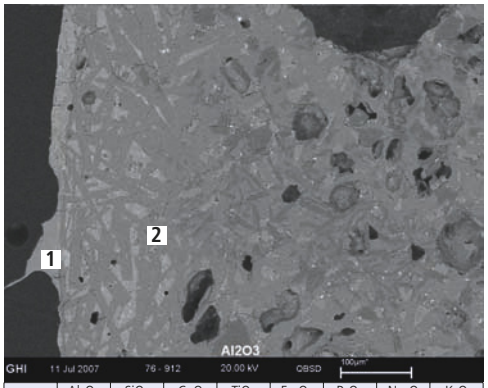

	Al_2O_3	SiO_2	CaO	TiO_2	Fe_2O_3	P_2O_5	Na_2O	K_2O
[1]	10,5	48,7	22,2	3,3	6,1	2,6	5,0	1,6
[2]	35,5	41,9	22,0	--	--	--	--	0,6

Fig. 11 SEM micrograph: High alumina refractory with mullite bonding after slag corrosion, overview of reaction zones at the hot face

Discussion and Conclusion

For the lining of waste incineration plants refractory SiC materials are mainly chosen for different parts of installation of the plants. Oxidation resistance of SiC refractories is therefore an essential criterion for the performance in such environments. In these studies the relation between measurable oxidation resistance and the composition of the bonding phase becomes obvious. The oxidation resistance was tested according to a standardized testing method and could be reapproved due to the use of materials which have already been applied to industrial plants. Their performance was also known and the laboratory results could be compared to the practical experiences in a plant. Beside measurable properties like volume and weight change or porosity the macroscopic examination in regard of crack formation is an also important criterion for the oxidation resistance. A qualitative assessment becomes obligatory.

In regard of the corrosion behaviour the extremely different oxidation resistance of the nitride bonded silicon carbide refractories becomes obvious. The scatter in the properties and microstructure of materials with the same nitride bonding type are remarkable. The SEM analysis underlines the importance of a homogenous nitride bonding phase in regard to a good oxidation resistance.

One conclusion concerning the corrosion behaviour in steam atmospheres is that the examined nitride-bonded silicon carbide materials show a very different oxidation resistance. Further the importance of a homogenous and effective formed bonding phase is pointed out by the SEM analyses of material A and B. As soon as an insufficient development of the nitride phase has taken place an inadequate oxidation resistance is a consequence. Fine silicon carbide grains are oxidised followed by the precipitation of a glassy silica-rich phase and cristobalite. In case of material B this results in stresses in the microstructure and microcracks. The experiments underline that at these conditions silicon-nitride phase has a higher oxidation resistance than silicon carbide. Passivating silica layers have not been examined since the oxidation rates within the steam atmosphere are too high. Lower gains in weight and volume, no crack formation as well as an oxidation resistant Si-O-N-phase are the conclusion in case of material A.

Permeability of corrosive constituents of the hot vapour phase could be underlined by the

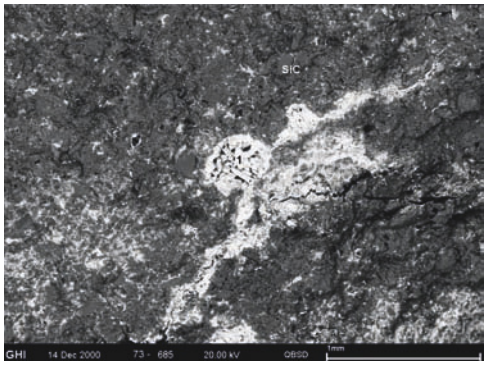

Fig. 10 Refractory SiC mortar after salt corrosion tests at 350 °C/500 h, detail of a pore filled with salt and crack formation

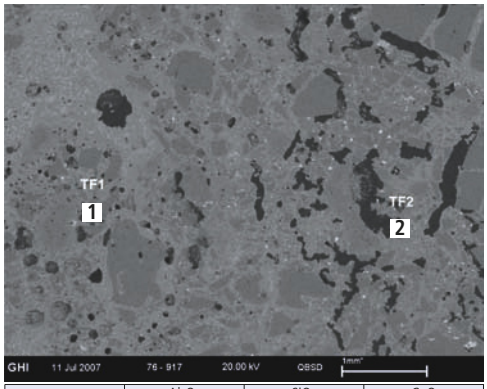

	Al_2O_3	SiO_2	CaO
[1]	55,6	30,4	13,9
[2]	70,8	22,1	7,1

Fig. 12 SEM micrograph: High alumina refractory with mullite bonding after slag corrosion, transition zone to porous microstructure with homogenous distribution of zircon (TF 2)

hot gas corrosion experiments. Infiltration and condensation of the salt compounds reveal a high potential for the corrosion and following degradation of the refractory material. On one hand high open porosity leads to the total penetration of these areas resulting in corrosion reaction respectively. On the other hand the microstructure changes intensively. Therefore high stresses and densified zones or crack formation due to condensation and precipitation of phases are a consequence. Filling of total pore areas with salt compounds are one example. Examinations of the high alumina refractory after operation in non-cooling areas of the vessel resulted as follows. XRD of the material as received showed a regular mineral composition of corundum, mullite, zircon and carnegieite ($NaAlSiO_4$). After operation the mineral composition changes leading to the following phases. At the hot face: Anorthite and hedenbergite ($CaFeSi_2O_6$), at the cold face: ZrO_2. Dissolution of zircon at the hot face and decomposition of zircon in related microstructure of the cold face are remarkable [7]. Following microstructural changes occur due to corrosion and totally penetration of the porous microstructure by the slag: Densification and decrease of porosity at the hot face. Related microstructure of the cold face porosity is increasing. These changes of the microstructure, and the phase formation due to the totally penetration of the brick by slag result in damages of the lining. The gradient of the different porosity areas and phase formations lead to a changed high temperature behaviour such as thermal expansion. Different thermal expansion coefficients result in stresses within the bricks and the lining. Spalling and deformation could be consequences.

References

[1] Köhne, V., Knorth, H., Pötsch, H.D.: VGB Kraftwerkstechnik 68 1(988) [12] 1279–1286

[2] Völker, W: Proc. 40. Internat. Colloquium on Refractories, Aachen 1997, pp. 174–175

[3] Mulch, St., Elstner, I., Grimm, D., Kinne, H.: VGB Kraftwerkstechnik 78 (1998) [3] pp. 70–74

[4] Tonnesen, Th., Breuers, M., Telle, R.: Proc. 47. Internat. Colloquium on Refractories, Aachen 2004, pp. 214–218

[5] Tonnesen, Th., Goerenz, E., Telle, R.: Refractories Manual (2007) 14–18

[6] ASTM C 863-83 (reapproved 1988): Standard Practice for Evaluating Oxidation Resistance of Silicon Carbide Refractories at Elevated Temperatures

[7] Kaiser, A., Telle, R., Lobert, M.: Proc. 10. Unified International Technical Conference on Refractories (UNITECR), Dresden 2007, pp. 272–275